Molecularly imprinted polymer chemosensor for selective determination of an *N*-nitroso-L-proline food toxin

Patrycja Lach,[a] Piyush Sindhu Sharma,[a] Karolina Golebiewska,[a] Maciej Cieplak,[a,*] Francis D'Souza,[b,*] and Wlodzimierz Kutner[a,c,*]

[a] *Institute of Physical Chemistry, Polish Academy of Sciences, Kasprzaka 44/52, 01-224 Warsaw, Poland*
[b] *Department of Chemistry, University of North Texas, 1155 Union Circle, #305070, Denton, TX 76203-5017, USA*
[c] *Faculty of Mathematics and Natural Sciences, School of Sciences, Cardinal Stefan Wyszynski University in Warsaw, Woycickiego 1/3, 01-815 Warsaw, Poland*

Corresponding Authors
Wlodzimierz Kutner – wkutner@ichf.edu.pl
Maciej Cieplak – mcieplak@ichf.edu.pl
Francis D'Souza – Francis.DSouza@UNT.edu
Tel.: +48 22 343 3188 (M. Cieplak)
Fax: +48 22 343 3333 (M. Cieplak)

Abstract

A molecularly imprinted polymer- (MIP) based chemosensor for selective determination of a chosen nitrosamine toxin, *N*-nitroso-L-proline (Pro-NO), was devised and fabricated. A polymer of phenol-substituted bithiophene molecularly imprinted with Pro-NO was deposited as a thin film on a Pt disk electrode surface and a gold film electrode of a quartz crystal resonator. With DFT computing, we modeled a structure of pre-polymerization (functional monomer)-template complex. Then, this complex was potentiodynamically electropolymerized to form an MIP-(Pro-NO) film on the electrode. Next, to vacate its imprinted cavities, the Pro-NO template was extracted from the MIP-(Pro-NO) with 0.1 M NaOH. Piezoelectric microgravimetry (PM) at EQCM and electrochemical (DPV and EIS) techniques were used to transduce binding of Pro-NO to molecular cavities of the MIP-(Pro-NO). With DPV and EIS chemosensing, the limits of detection (LOD) were ~81 nM and 36.9 nM Pro-NO; and the selectivity coefficient for the urea, glucose, creatinine, and adrenalin interference was 6.6, 13.2, 2.1, 2.0, and 2.3, 2.0, 3.3, 2.5, respectively. With PM under flow injection analysis (FIA) conditions, the LOD was 10 μM Pro-NO. The MIP-(Pro-NO) chemosensor detectability and selectivity with respect to interferences were sufficiently high to determine Pro-NO in the protein-providing food products.

Keywords

Molecularly imprinted polymer (MIP), conducting materials, polybithiophene, sensor, food toxin.

1. Introduction

Public awareness of hazardous chemicals in food has grown tremendously in recent years. Therefore, the demand for safe food is great. Consumers continuously express concerns about health risks because of toxins in food products. Thus, legislature and health authorities as well as companies operating in the food market require adequate toxin determination protocols that are efficient, sensitive, selective, fast, inexpensive, and suitable for sample mass screening analytical procedures.

Origins of food toxicity are many. Certain processing conditions may generate toxic compounds. For instance, heterocyclic aromatic amine [1] and *N*-nitrosamine [2] toxic compounds appear in protein-providing food products such as meat, fish, poultry, and eggs, if these are fried, broiled, or grilled at high temperatures. Moreover, smoke contains these compounds. Often, continuous exposures to low doses of these toxins cause various chronic diseases, serious hormonal dysfunctions, and cancer [3].

Methods currently used to determine these toxins, for instance solid-phase extraction (SPE) coupled with (gas chromatography)-(mass spectrometry), GC-MS, [4] and high performance liquid chromatography (HPLC), [5] are either expensive or tedious and time-consuming.

Therefore, fast, inexpensive, and reliable ways to determine these toxins in food matrices are necessary. An appealing way to execute these procedures is to use biosensors or chemical sensors, i.e., chemosensors, [6]. Although biosensors are often specific, they suffer from low stability of their natural recognition units and high cost. In contrast, chemosensors are stable and inexpensive although they are selective rather than specific. These chemosensors are suitable for both monitoring toxins in food products and for point-of-care disease diagnostics.

In the present research, a chemosensor using a polymer molecularly imprinted with *N*-nitroso-L-proline **1**, MIP-(Pro-NO), a food toxin, was devised and fabricated. Generally, molecular imprinting involves polymerization of a pre-polymerization complex in solution of functional monomers with a template, which is often the analyte itself, in the presence of cross-linking monomers. Subsequent removal of this template leaves in the resulting polymer molecular cavities complementary in their size and shape to those of the template molecules. Moreover, orientations of recognition sites of these cavities match those of the binding sites of the template molecules. Stability constants of complexes of these molecular cavities, i.e., artificial receptors, with analyte molecules are often similar to those of the biological receptors. Therefore, MIP-based chemosensors are promising tools for food safety control [7]. Recently, a

silica gel coated with tobacco-specific nitrosamines (TSNAs) imprinted polymer (SiO_2/MIP) was applied successfully for fabrication of improved cigarette filters [8]. Filters with SiO_2/MIP lowered concentration of different TSNAs in cigarette smoke to 41 – 18% of the values typical for most cigarettes; thus the need for chemosensors for these toxins. Toward end, we herein have devised a chemosensor for selective determination of Pro-NO in food products of animal origin. We deposited a film of an MIP imprinted with Pro-NO on a Pt disk electrode and a gold film electrode of a quartz crystal resonator (Au-QCR). These transducers were then used for electrochemical (DPV and EIS) and piezoelectric microgravimetry (PM), respectively, selective determination of the nitrosamine toxin.

2. Materials, instrumentation, and procedures

2.1 Materials and reagents

All chemicals and solvents were from Sigma-Aldrich except for *N*-nitroso-L-proline, which was from Toronto Research Chemicals, Inc.

2.2 Instrumentation

A computerized electrochemistry system of AUTOLAB, composed of PGSTAT12 potentiostat/galvanostat equipped with a FRA2 frequency response analyzer and controlled by GPES 4.9 software, all from the same manufacturer (Eco Chemie), were used for the CV, DPV, and EIS measurements. In these measurements, a three-electrode one-compartment V-shaped glass electrochemical mini cell was used. A 1-mm diameter Pt disk sealed in soft glass tubing, an Ag/AgCl, and a coiled Pt wire were the working, pseudo-reference, and counter electrode, respectively.

A model EQCM 5610 [9] and EQCM 5710 [10] electrochemical quartz crystal microbalance (EQCM) driven by EQCM 5710-S2 software, all of the Institute of Physical Chemistry of the Polish Academy of Sciences (IPC PAS), were used to deposit by multicyclic potentiodynamic electropolymerization and to conduct simultaneously PM measurements under FIA conditions. The resonant frequency change was measured with 1-Hz resolution using 14-mm diameter, AT-cut, plano-plano, Au-QCRs of 10-MHz resonant frequency with 5-mm diameter Au disk film electrodes deposited on both crystal sides. A coiled Pt wire and an AgCl film-coated Ag wire functioned as the counter and pseudo-reference electrode, respectively. For electropolymerization, the EP-20 potentiostat of IPC PAS was interfaced with the EQCM 5710 microbalance whose Au-QCR holder was mounted horizontally such that its resonator cavity formed a small-volume electrochemical cell. The cell was filled with a 200-µL sample of the solution for electropolymerization, and both the Pt counter pseudo-

reference electrodes were then immersed in this solution.

The (Pro-NO)-extracted MIP-(Pro-NO) films deposited on Au-QCRs were used for Pro-NO determination by PM under FIA conditions. The 0.1 M phosphate buffer, PB, (pH = 7.0) carrier solution was pumped at the 35 μL/min flow rate through the EQCM 5610 holder with a model NE-500 syringe pump driven by the WinPumpTerm software of New Era Pump Systems. The 100-μL samples of the Pro-NO test solutions were injected with a model 7725i rotary six-port valve of Rheodyne. Composition of the Pro-NO test solutions was the same as that of the carrier solution.

The UV-vis spectra were recorded with 0.1-nm resolution using a UV-2550 spectrophotometer controlled by UVProbe 2.21 software of Shimadzu Corp.

The infrared spectra of thin films were recorded using polarization-modulation infrared reflection-absorption spectroscopy (PM-IRRAS) with a Vertex 80v Fourier transform infrared (FTIR) spectrometer of Bruker, equipped with a PMA50 module of PM-IRRAS. The nitrogen-cooled MCT (Hg-Cd-Te) detector reached a reasonably high signal-to-noise ratio. All IR spectra were analyzed with OPUS 6.5 software of Bruker.

The MIP-(Pro-NO) films were imaged with AFM (in the Tapping™ mode) using a MultiMode 8 AFM microscope of Bruker under control of a Nanoscope V controller. The films for imaging were deposited on Au-film coated glass slides.

The XPS spectra were recorded on a PHI 5000 VersaProbe (ULVAC-PHI) scanning ESCA microprobe using monochromatic Al Kα radiation ($h\nu$ = 1486.6 eV). The Casa XPS software then evaluated the XPS data. Background was subtracted using the Shirley method and peaks were fitted with (Gaussian-Lorentzian)-shaped profiles. The binding energy (*BE*) scale was referenced to the C 1s peak with *BE* = 284.6 eV.

2.3 Procedures

Syntheses of the functional monomer, *p*-bis(2,2'-bithien-5-yl)methylphenol **2**, and the cross-linking monomer, 5,5′,5″-methanetriyltris(2,2′-bithiophene) **3**, were described elsewhere [11].

2.3.1 Synthesis of the MIP-(Pro-NO) film

The MIP-(Pro-NO) film was prepared by oxidative electropolymerization under potentiodynamic conditions with five potential cycles over the potential range of 0 to 1.30 V at the potential scan rate of 50 mV/s. An acetonitrile solution of 50 μM Pro-NO **1**, 100 μM *p*-bis(2,2'-bithien-5-yl)methylphenol **2**, 500 μM 5,5′,5″-methanetriyltris(2,2′-bithiophene) **3**, and 100 mM tetrabuthylammonium perchlorate was used for this electropolymerization. Before

MIP-(Pro-NO) film deposition, the electrode was cleaned in a "piranha" solution for 10 min, and then mirror finished with 0.05 µm alumina slurry. (*Warning. The "piranha" solution is very dangerous if it comes in contact with skin or eyes.*)

For XPS and PM-IRRAS measurements as well as AFM imaging, MIP-(Pro-NO) films were deposited on Au film-coated glass slides using a homemade holder with a Pt plate as the counter electrode and an Ag/AgCl as the pseudo-reference electrode. The working and counter electrodes were mounted in parallel at a distance of ~5 mm.

2.3.2 Synthesis of the control non-imprinted polymer (NIP) film

The NIP film was prepared by oxidative electropolymerization under the same conditions as those used for MIP-(Pro-NO) synthesis but without template **1** addition.

2.3.3 Pro-NO template extraction from the MIP-(Pro-NO) film

After electropolymerization, the Pro-NO template was extracted from the MIP-(Pro-NO) film by immersing the film-coated electrode in 0.1 M NaOH for 30 min at room temperature.

2.3.4 Electrochemical measurements

All DPV and EIS measurements were performed at room temperature, (20±1)°C, using the electrochemical mini cell described in Section 2.2, above, and the PB (pH = 7.0) solution of the 100 mM $K_3[Fe(CN)_6]$ and 100 mM $K_4[Fe(CN)_6]$ redox probe.

In the DPV measurements, potential was scanned from 0 to 0.6 V vs. Ag/AgCl with the potential step of 5 mV. The amplitude of 50-ms pulses applied was 25 mV.

In the EIS experiments, an ac excitation signal of frequency in the range of 1 MHz to 100 mHz and 10-mV sinusoidal amplitude was used at open-circuit potential. The electrochemical system was approximated with a modified Randles-Ershler equivalent circuit, $R_s+CPE/(R_{ct}+W_o)$, with Z-View software (Scriber Associates, Inc.) where R_s, R_{ct}, *CPE*, and W_o are solution resistance, charge transfer resistance, constant phase element, and Warburg impedance, respectively.

After each Pro-NO determination, the MIP-(Pro-NO) film coated electrode was immersed in 0.1 M NaOH for 10 to 30 min at room temperature, under magnetic stirring, until all the mobile Pro-NO analyte was extracted, as confirmed by a stable DPV peak of ~6 µA for the redox probe.

2.3.5 Piezomicrogravimetric measurements

For piezomicrogravimetric measurements, the MIP-(Pro-NO) film was deposited on the Au-

QCR by potentiodynamic electropolymerization. Curves of the dependence of current, resonant frequency change, and dynamic resistance change on potential were recorded simultaneously during electropolymerization. The decrease of resonant frequency corresponded to the increase of the Au-QCR mass due to deposition of the MIP-(Pro-NO) film. A small (~50 Ω) change in dynamic resistance accompanying MIP-(Pro-NO) film deposition evidenced film rigidity, and only negligible influence of its viscosity and density changes on the total frequency change.

2.3.6 Preparation of grilled meat samples

Pro-NO was also determined in grilled pork neck samples that were purchased in a local butcher shop, grilled, and then blended with water. Next, a solution of 0.1 M in PB (pH = 7.0), 0.1 M in $K_3[Fe(CN)_6]$ and 0.1 M in the $K_4[Fe(CN)_6]$ redox probe was added, and the sample was sonicated for 10 min. Subsequently, the sample was centrifuged for 15 min at 4 C, and the supernatant was then collected. Finally, the sample was spiked with a known amount of Pro-NO.

3. Results and discussion

3.1 Choice of a functional monomer

Molecular imprinting involves, first, preorganization of functional monomer molecules around a template molecule to form a pre-polymerization complex. This self-assembly is crucial for successful imprinting. That is, the complex should be stable to survive subsequent polymerization and to afford desired selectivity; and it should be sufficiently labile to enable template removal from the resultant MIP-(Pro-NO). Therefore, the choice of proper functional monomers is very important. Toward that end, computational DFT modeling at the B3LYP/6-31G(d) level of complex formation was performed for two functional monomers, vis., *p*-bis(2,2'-bithien-5-yl)methyl-*o*-catechol and (*p*-bis(2,2'-bithien-5-yl)methylphenol **2**; and two templates, vis., the *N*-nitroso-L-proline **1** and a *N*-acetyl-L-proline, nontoxic "dummy" template. Structure of the latter is very similar to that of the *N*-nitroso-L-proline (Table S1 and Scheme S1, Supporting Information). The (functional monomer)-to-template mole ratio was 2 : 1. To confirm that the "dummy" template was properly selected, the structure of the complex of *N*-acetyl-L-proline with *p*-bis(2,2'-bithien-5-yl)methyl-o-catechol was optimized. Next, bithienyl moieties of the complex were "frozen", and then the *N*-acetyl-L-proline molecule was exchanged with target analyte **1**. Finally, Gibbs free energy change, ΔG, which corresponds to **1** binding to the imprinted molecular cavity, was calculated using DFT.

Calculations revealed that the highest negative gain of ΔG was for *p*-bis(2,2'-bithien-5-yl)methyl-*o*-catechol (-278 kJ/mol). Moreover, the ΔG value for analyte interacting with the cavity generated with the "dummy" template was even higher (-296 kJ/mol). The ΔG for complex formation of Pro-NO with functional monomer **2** was significantly lower (-130 kJ/mol) but still sufficiently high to form a stable complex (Scheme 1).

[Here Scheme 1]

At an early stage of the present research, we tested the usefulness of different functional monomers and templates for MIP preparation. Despite very promising results of DFT calculations (ΔG = -278.2 kJ/mol), the MIP chemosensor prepared with the *p*-bis(2,2'-bithien-5-yl)methyl-*o*-catechol functional monomer and *N*-acetyl-L-proline "dummy" template (Fig. S1a) was not selective in DPV determinations. Most likely, the presence of two binding sites in each functional monomer molecule was the reason why they were able to adjust their conformation in the imprinted cavity and, therefore, to bind efficiently not only molecules of the target analyte but also those of interferences of similar structures. Likewise, selectivity of the MIP chemosensor prepared with the *p*-bis(2,2'-bithien-5-yl)methylphenol **2** functional monomer and the *N*-acetyl-L-proline "dummy" template (Fig. S1c), much higher but still unsatisfactory, confirmed this inference. The best geometric fit of the imprinted cavity to analyte **1** and, therefore, the highest selectivity was reached for the MIP film prepared using template **1** and functional monomer **2.** (See Section 3.5, below). Therefore, these were used in subsequent investigations.

Stoichiometry and stability of the DFT optimized structure of the pre-polymerization complex of **1** with **2** was confirmed by UV-vis titration (Fig. S2a). By plotting absorbance of the functional monomer **2** at 320 nm wavelength against the Pro-NO concentration (Fig. S2a, inset), we determined stoichiometry of this complex to be 2 : 1. The stability constant, K_s, of this complex was determined with the Scatchard method using Eq. 1,

$$\frac{(A - A_0)}{2c^2_{(\mathrm{Pro-NO})}} = -K_s(A - A_0) + K_s c_{(\mathrm{FM})_0} \Delta\varepsilon_{[2(\mathrm{FM})-(\mathrm{Pro-NO})]} \qquad (1)$$

where A_0 and A stand for the absorbance of functional monomer **2** before and after addition of Pro-NO, respectively. The $c_{(\mathrm{FM})_0}$ symbol represents the initial concentration of the functional monomer, equaling 31.25 μM. The dependence of $\Delta\varepsilon_{[2(\mathrm{FM})-(\mathrm{Pro-NO})]} = \varepsilon_{[2(\mathrm{FM})-(\mathrm{Pro-NO})]}$ -

$\varepsilon_{(FM)}$ - $\varepsilon_{(Pro-NO)}$ combines the $\varepsilon_{[2(FM)-(Pro-NO)]}$, $\varepsilon_{(FM)}$, and $\varepsilon_{(Pro-NO)}$ symbols, and denotes molar absorptivity of the [2(FM)-(Pro-NO)] complex, functional monomer **2**, and Pro-NO analyte, respectively. According to Eq. 1, we plotted $A - A_0/2c^2_{(Pro-NO)}$ as a function of $A - A_0$ and, from the slope of the straight line obtained, we determined the K_s value of $(3.14\pm0.71) \times 10^9$ M^{-2} (Fig. S2b). This quite high value confirmed formation of a stable pre-polymerization complex.

3.2 Preparation of the polymer molecularly imprinted with Pro-NO

An acetonitrile solution of Pro-NO **1** and functional monomer **2,** at the 1 : 2 mole ratio, and excess of cross-linking monomer **3** were used for oxidative electropolymerization under potentiodynamic conditions on the Pt disk electrode (Fig. 1a). A pronounced anodic peak current increase in consecutive cycles confirmed that the deposited polymer film was highly conductive. Moreover, Au-QCRs were coated with MIP-(Pro-NO) films the same way (Fig. S3). Changes of resonant frequency and dynamic resistance were quite well-developed only in the 1.0 to 1.3 V potential range. In this range, all monomers were electro-oxidized. Moreover, these changes were very similar in each subsequent cycle. This means that an MIP-(Pro-NO) layer of similar mass was deposited in each potential cycle. The overall resonant frequency change of -3677.7 Hz corresponds to the deposited film mass of 3.19 μg, as determined using Sauerbrey's equation.

[Here Figure 1]

3.3 Confirmation of template removal from MIP-(Pro-NO)

The Pro-NO template was extracted from its molecular cavity by immersing the MIP-(Pro-NO) film coated electrode in 0.1 M NaOH until the DPV peak of the chemosensor reached a constant value. Apparently, the presence of Pro-NO in the MIP-(Pro-NO) film hampered diffusion of the $[Fe(CN)_6]^{2+}/[Fe(CN)_6]^{3+}$ redox probe towards the electrode (Curve *1* in Fig. 1b). However, this diffusion was enabled after Pro-NO extraction from the film for different time spans (Curves *2* and *3* in Fig. 1b). Electrode activity of the $Fe(CN)_6^{2+}/Fe(CN)_6^{3+}$ redox couple did not increase any more after 20-min extraction. Therefore, the Pro-NO template was extracted for 20 min before further experiments.

Extraction of the Pro-NO template was confirmed by XPS and PM-IRRAS measurements. The XPS spectrum recorded for the MIP-(Pro-NO) film deposited on the gold-coated glass slide showed two N 1s peaks at ~398 and ~400 eV (Fig. S4a). That way,

Pro-NO template imprinting in the MIP-(Pro-NO) was confirmed because Pro-NO was the only nitrogen source in the film. These signals were, however, absent after extraction of the Pro-NO template (Fig. S4b). Moreover, changes in the PM-IRRAS spectra in the range of 1700-1500 cm^{-1} and 1500-1300 cm^{-1} of the MIP-(Pro-NO) film before and after template extraction indicated template removal (Fig. S5).

3.4 AFM characterization of the polymer molecularly imprinted with Pro-NO

The MIP-(Pro-NO) film was AFM imaged to unravel its morphological differences before and after template extraction (Fig. S6). Apparently, the MIP-(Pro-NO) surface was discontinuous and quite irregular, in that it consisted of 20- to 60-nm polymer grains. Moreover, the AFM determined roughness and thickness of the MIP-(Pro-NO) film was 29.3 nm and 154±8 nm, respectively, before Pro-NO template extraction. After Pro-NO extraction, this roughness and thickness changed only slightly, being 26.2 nm and 161±5 nm, respectively.

3.5 Characterization of the MIP-(Pro-NO) electrochemical sensor for determination of Pro-NO

Two electroanalytical techniques were used to operate the Pro-NO chemosensors. That is, the DPV (Fig. 2) and EIS curves (Fig. 3) were consecutively recorded at the template-extracted MIP-(Pro-NO) film coated electrode after addition of a known amount of the Pro-NO analyte to the $K_4Fe(CN)_6/K_3Fe(CN)_6$ redox probe solution. The experiments were performed under stagnant-solution conditions.

The DPV peak for the redox probe at the MIP-(Pro-NO) film-coated Pt disk electrode decreased more pronouncedly the higher was the Pro-NO concentration in solution (Fig. 2a). Moreover, charge transfer resistance simultaneously increased. Apparently, redox probe diffusion through the MIP-(Pro-NO) film was slowed when target analyte molecules entered the film. The DPV peak linearly decreased with the increase of Pro-NO concentration in the range of 9.1 to 43.9 µM (Fig. 2b), thus obeying the linear regression equation of $I_{DPV,0} - I_{DPV,s}$ /µA = 3.053/µA + 0.094 $c_{(Pro\text{-}NO)}$/µM with the correlation coefficient, $R^2 = 0.9708$. The limit of Pro-NO detection was LOD = 80.9 nM at S/N = 3. Moreover, the chemosensor was highly selective. That is, it did not respond at all to urea, glucose, and adrenalin interference. Even with respect to creatinine, a compound of different chemical composition but with almost identical space arrangement of functional groups as that of **1**, the MIP-(Pro-NO) chemosensor was selective. The selectivity coefficient for urea, glucose, creatinine, and adrenalin was 6.6, 13.2, 2.1, and 2.0, respectively.

[Here Figure 2]

In the EIS measurements (Fig. 3a), the linear dynamic concentration range of 9.1 to 43.9 μM Pro-NO satisfies the linear regression equation of ΔR_p /Ω = 112.455/Ω + 8,651 $c_{(Pro\text{-}NO)}$ /μM with the correlation coefficient, $R^2 = 0.9965$. The LOD for Pro-NO was 36.9 nM. The selectivity coefficient for urea, glucose, creatinine, and adrenaline was 2.3, 2.0, 3.3, and 2.5, respectively.

[Here Figure 3]

3.6 Characterization of the MIP-(Pro-NO) PM chemosensor for determination of Pro-NO under FIA conditions

Flow injection analysis (FIA) is a very powerful tool for rapid and accurate determination of analytes in many samples of high throughput. For that purpose, we used PM transduction. Changes of resonant frequency with time, incurred by injections of Pro-NO samples, are shown in Figure 4. The linear dynamic concentration range (Fig. 4, inset) of 0.125 to 2.0 mM satisfies the linear regression equation of Δf /Hz = -0.928/Hz – 2.305 $c_{(Pro\text{-}NO)}$ /mM with the correlation coefficient, $R^2 = 0.9886$. The LOD for Pro-NO was 10 μM. The NIP film coated Au-QCR response to the Pro-NO was nearly independent of the Pro-NO concentration (Fig. 4, inset). Hence, the determined very high impact factor, IF > 20, confirmed that molecular cavities of a very well defined structure and high affinity to the target analyte molecules were imprinted.

[Here Figure 4]

3.7 Determination of Pro-NO in grilled pork neck

To confirm that detectability of our chemosensor is sufficient for real food sample analysis, we determined Pro-NO in grilled pork neck samples. After the sample spiking with Pro-NO, DPV determinations were performed for that purpose. The DPV peaks for different Pro-NO concentrations were normalized with respect to that for the first spike of the lowest concentration. Then, recovery was determined (Table 1). The Pro-NO concentrations determined in the samples compared to those prepared.

[Here Table 1]

4. Conclusions

We devised and fabricated an electrochemical MIP-(Pro-NO) chemosensor for selective determination of *N*-nitroso-L-proline at concentrations lower than the concentrations typical for smoked or fried animal food products. Cured meat products contain *N*-nitroso-L-proline at levels of up to 360 μg/kg [12]. Many countries have no directives concerning the maximum permitted *N*-nitrosamine content in food. Usually, this content is regulated by limits imposed on the amount of nitrite added to meat in the course of processing. In the European Union, the maximum permitted concentration of nitrite in processed meat is 150 mg/kg [13].

The herein Pro-NO imprinting, and then releasing from the MIP-(Pro-NO) were confirmed by DPV, XPS, and PM-IRRAS measurements.

The DPV and EIS response of the MIP-(Pro-NO) chemosensor to Pro-NO was linear in the concentration range of 9.09 to 43.86 μM with the LOD for Pro-NO of 80.85 nM and 36.9 nM, respectively. The PM signal measured under FIA conditions was linear in the range of 0.125 to 2.0 mM with the LOD of 10 μM. Moreover, a very high imprinting factor exceeding 20 strongly indicated that the imprinting was very successful. Apparently, this imprinting resulted in very well defined molecular cavities of high affinity to Pro-NO molecules.

In DPV determinations, selectivity of the MIP-(Pro-NO) chemosensor with respect to urea and glucose, i.e., interferences much different from the analyte, was high. However, it was lower to creatinine and adrenalin, the compounds of a very similar size, shape, and space arrangement of functional groups.

Successful determination of Pro-NO in real meat samples indicates that the MIP-(Pro-NO) chemosensor is a promising tool for this toxin determination in food samples of animal origin. Toxin determinations like those performed within the present research will alleviate consumer concerns for food safety as well as will exert a positive impact on food distribution and sale.

Acknowledgments

We acknowledge the Polish National Science Foundation (Grant NCN No. 2014/15/B/NZ7/01011 to W.K.) and UNT-AMMPI for financial support.

References

[1] a) J. Gauvin, S. Broyde and R. Shapiro, *Chem Res Toxicol* **2001**, *14*, 476-482; b) K. Wakabayashi, M. Nagao, H. Esumi and T. Sugimura, *Cancer. Res.* **1992**, *52*, 2092s-2098s; c) H. A. Schut and E. G. Snyderwine, *Carcinogenesis* **1999**, *20*, 353-368.

[2] S. S. Herrmann, L. Duedahl-Olesen and K. Granby, *Food Control* **2015**, *48*, 163-169.

[3] a) J. D. Adams, S. J. Lee and D. Hoffmann, *Carcinogenesis* **1984**, *5*, 221-223; b) S. S. Hecht and D. Hoffmann, *Carcinogenesis* **1988**, *9*, 875-884; c) S. Ventanas and J. Ruiz, *Talanta* **2006**, *70*, 1017-1023.

[4] a) C. J. Smith, X. Qian, Q. Zha and S. C. Moldoveanu, *J. Chromatogr. A* **2004**, *1046*, 211-216; b) R. Andrade, F. G. R. Reyes and S. Rath, *Food Chemistry* **2005**, *91*, 173-179.

[5] N. V. Komarova and A. A. Velikanov, *J. Anal. Chem.* **2001**, *56*, 359-363.

[6] R. H. Farahi, A. Passian, L. Tetard and T. Thundat, *Acs Nano* **2012**, *6*, 4548-4556.

[7] P. L. Wang, X. H. Sun, X. O. Su and T. Wang, *Analyst* **2016**, *141*, 3540-3553.

[8] M. T. Li, Y. Y. Zhu, L. Li, W. N. Wang, Y. G. Yin and Q. H. Zhu, *J Sep Sci* **2015**, *38*, 2551-2557.

[9] A. Kochman, A. Krupka, J. Grissbach, W. Kutner, B. Gniewinska and L. Nafalski, *Electroanalysis* **2006**, *18*, 2168-2173.

[10] W. Koh, W. Kutner, M. T. Jones and K. M. Kadish, *Electroanalysis* **1993**, *5*, 209-214.

[11] a) M. Sosnowska, P. Pieta, P. S. Sharma, R. Chitta, B. K. Chandra, V. Bandi, F. D'Souza and W. Kutner, *Anal. Chem.* **2013**, *85*, 7454-7461; b) T. P. Huynh, M. Sosnowska, J. W. Sobczak, C. B. Kc, V. N. Nesterov, F. D'Souza and W. Kutner, *Anal. Chem.* **2013**, *85*, 8361-8368.

[12] C. Crews in *Processing Contaminants: N-Nitrosamines*, *Vol. 2* Eds.: Y. Motarjemi, G. Moy and E. Todd), Elsevier Inc., USA, **2014**, pp. 409-415.

[13] The_European_Parlament_and_The_Council_of_The_European_Union in *DIRECTIVE 2006/52/EC OF THE EUROPEAN PARLIAMENT AND OF THE COUNCIL*, *Vol.* Official Journal of the European Union, **2006**, pp. 10-22.

Table 1. The DPV peak current recorded at the MIP-(Pro-NO) film coated Pt disk electrode for grilled pork neck samples spiked with Pro-NO.

Sample No.	The DPV peak current at the MIP-(Pro-NO) film coated electrode ± std. dev., µA	Amount of Pro-NO added to a grilled pork neck samples, µM	Determined Pro-NO concentration ± std. dev., µM	Recovery ± std. dev., %
1.	11.69 ± 0.58	8.66	-	-
2.	12.78 ± 0.64	17.21	20.34 ± 6.82	118 ± 39
3.	13.23 ± 0.66	25.27	25.09 ± 7.05	98 ± 27
4.	13.64 ± 0.68	33.80	29.44 ± 7.27	87 ± 21
5.	13.93 ± 0.70	42.37	32.54 ± 7.43	77 ± 17

Scheme 1. Structural formulas of (a) the (*N*-nitroso-L-proline) template **1** the (*p*-bis(2,2'-bithien-5-yl)methylphenol) **2** functional monomer and the (5,5′,5″-methanetriyltris(2,2′-bithiophene) **3** cross-linking monomer and (b) the complex of **1** with two molecules of the functional monomer **2.** (c) The DFT optimized structure of the pre-polymerization complex in vacuum.

Figure 1. (a) Current-potential curves of 5-cycle potentiodynamic electropolymerization leading to deposition of an MIP-(PRO-NO) film on the 1-mm diameter Pt disk electrode from the acetonitrile solution of 50 µM Pro-NO **1**, 100 µM *p*-bis(2,2'-bithien-5-yl)methylphenol **2**, 500 µM 5,5′,5″-methanetriyltris(2,2′-bithiophene) **3**, and 100 mM tetrabuthylammonium perchlorate. (b) DPV curves recorded at the 1-mm diameter Pt disk electrode coated with the MIP-(Pro-NO) film in the presence of the redox probe, 0.1 M $K_3[Fe(CN)_6]$ and 0.1 M $K_4[Fe(CN)_6]$, in 0,1 M phosphate buffer (pH = 7.0) before (*1*) and after (*2*) template extraction for 10, (*3*) 20, and (*4*) 30 min.

Figure 2. (a) Changes in the DPV signal recorded for the MIP-(Pro-NO) film coated Pt disk electrode (*1*) after template **1** extraction with 0.1 M NaOH for 30 min as well as after addition of (*2*) 9.09, (*3*) 18.02, (*4*) 26.79, (*5*) 35.40 and (6) 43.86 µM Pro-NO. (b) Calibration plots for the MIP-(Pro-NO) film coated electrode for (*1*) Pro-NO, (*2*) creatinine, (*3*) adrenalin (*4*) urea, (*5*) glucose, and (*6*) Pro-NO at the NIP film coated Pt disk electrode. All experiments were performed in the presence of the redox probe, 0.1 M $K_3[Fe(CN)_6]$ and 0.1 M $K_4[Fe(CN)_6]$, in 0.1 M phosphate buffer (pH = 7.0).

Figure 3. (a) EIS spectra of the MIP-(Pro-NO) film coated Pt disk electrode (*1*) after template **1** extraction with 0.1 M NaOH for 20 min, and then after addition of (*2*) 9,09, (*3*) 18,02, (*4*) 26,79, (*5*) 35,40 and (6) 43,86 µM Pro-NO. (b) Calibration plots for (*1*) Pro-NO, (*2*) creatinine, (*3*) adrenalin, (*4*) urea, (*5*) glucose at the MIP-(Pro-NO) film coated Pt electrode and (*6*) Pro-NO at the NIP film coated Pt electrode. All experiments were performed in the presence of the redox probe, 0.1 M $K_3[Fe(CN)_6]$ and 0.1 M $K_4[Fe(CN)_6]$, in 0.1 M phosphate buffer (pH = 7.0).

Figure 4. Changes of resonant frequency with time resulting from injections of 150-µL Pro-NO samples under FIA conditions. The MIP-(Pro-NO) film was deposited on a 10-MHz Au-QCR. The flow rate of a 0.1 M phosphate buffer (pH = 7.0) carrier solution was 35 µL/min.

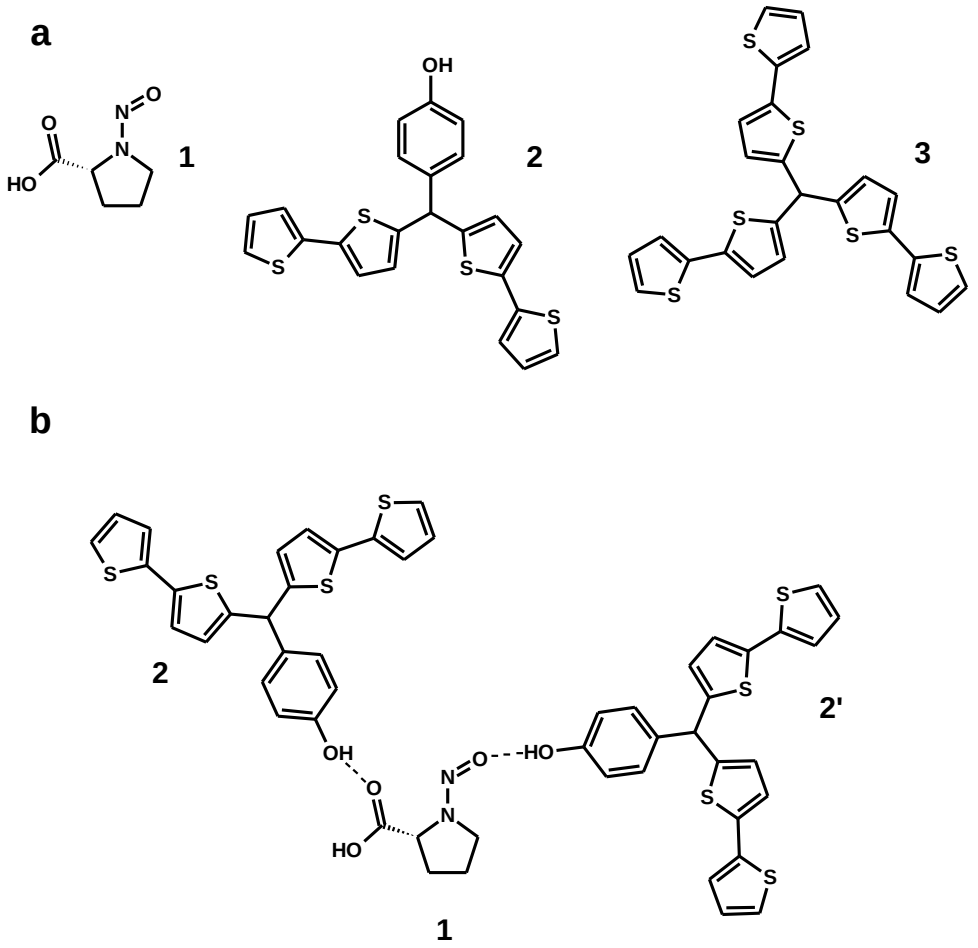

Scheme 1

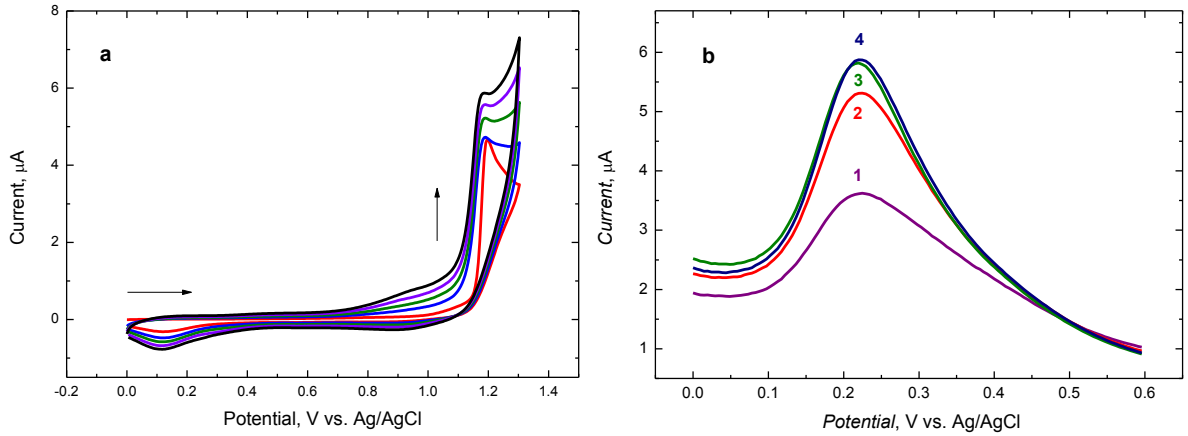

Figure 1

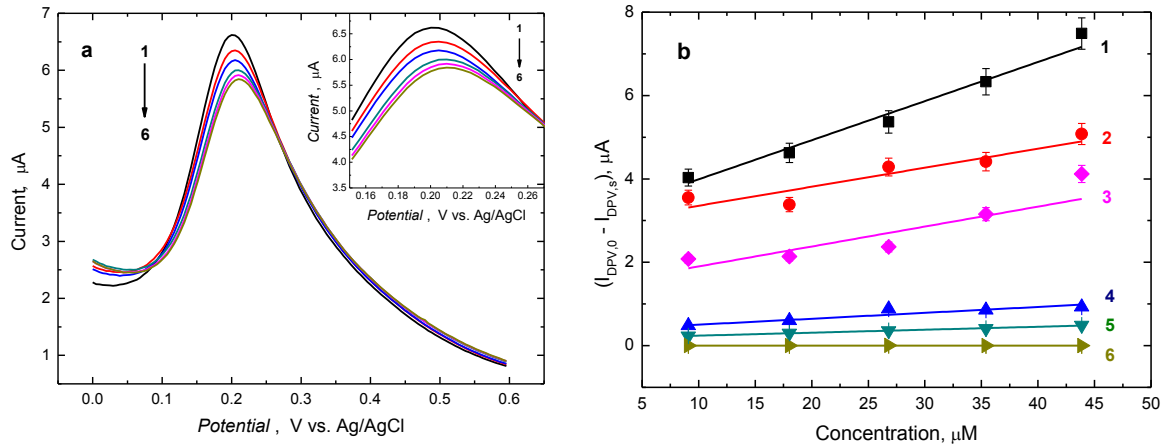

Figure 2

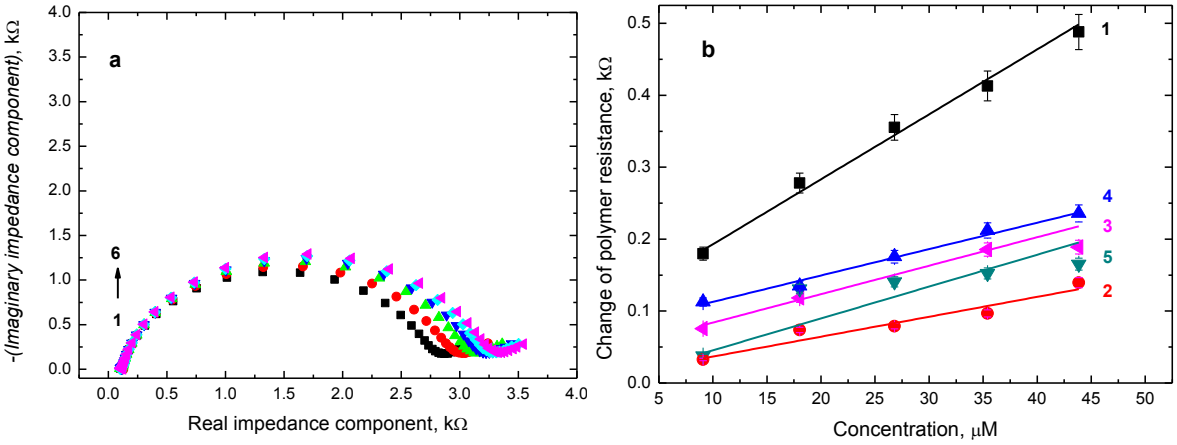

Figure 3

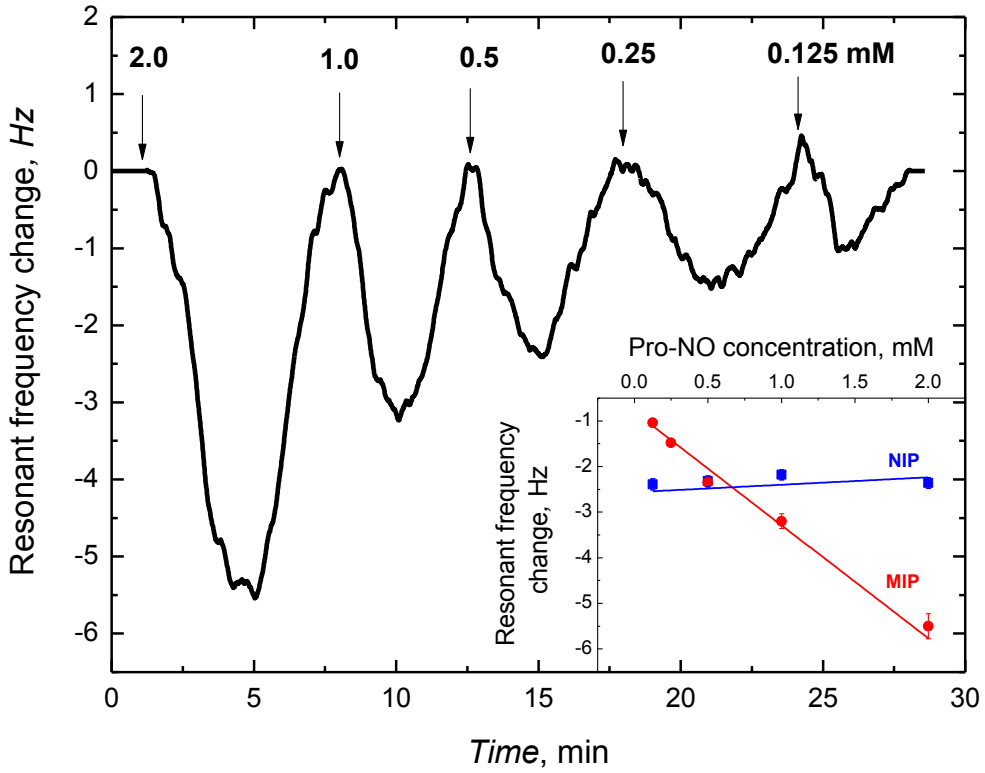

Figure 4